

## A Range Algorithm for Ground Penetrating Radar

Thurlow W. H. Caffey  
Sandia National Laboratories<sup>o</sup>  
P. O. Box 87185  
Albuquerque, NM 87185-0705  
Tel 505-844-4217 / Fax 505-844-0240 / twcaffe@sandia.gov

**Abstract** — A range-to-target algorithm for application to targets which exhibit a crude hyperbolic wiggle trace is described. The current practice is to use the apex time of the hyperbolic response together with an estimate of the propagation velocity to furnish the range. This new algorithm minimizes a difference function over a velocity search interval to provide the range. Examples for a variety of media, targets, range, and operating frequency are given for both simulated data and actual field data provided by others. Generally, the range is within 5% of the true value when known, or is consistent with values furnished by others.

### ASSUMPTIONS

Several assumptions are required for the development of the algorithm: The transmitter is not modulated during the pulse interval; the media between the radar and the target is homogeneous and isotropic; the round-trip travel time is measured during a linear traverse past the target; and the transmitting and receiving antennas of the GPR are appropriately separated.

### THE TRAVERSE

Suppose that the radar is translated in uniform increments along its own axis and approaches, illuminates, and passes-by a discrete target as shown in Fig. 1. If the maximum radius of curvature of the target is much less than the minimum range, the slant range is given by

$$R_i = 0.5vt_i, \quad (1)$$

where  $v$  is the velocity,  $t_i$  is the round trip time, and  $R_i$  is the slant range from the midpoint of the antenna separation distance  $2s$  at the  $i$ -th traverse position  $z_i$ . The minimum time is denoted by  $t_o$  and the corresponding traverse position is denoted by  $z_o$ . The minimum range is given by

$$R_o = 0.5vt_o. \quad (2)$$

The slant range from the midpoint can also be written as

REF ID: A6411  
MAR 11 1988  
(3)  
C 871

$$R_i = \sqrt{\rho^2 + z_i^2}. \quad (3)$$

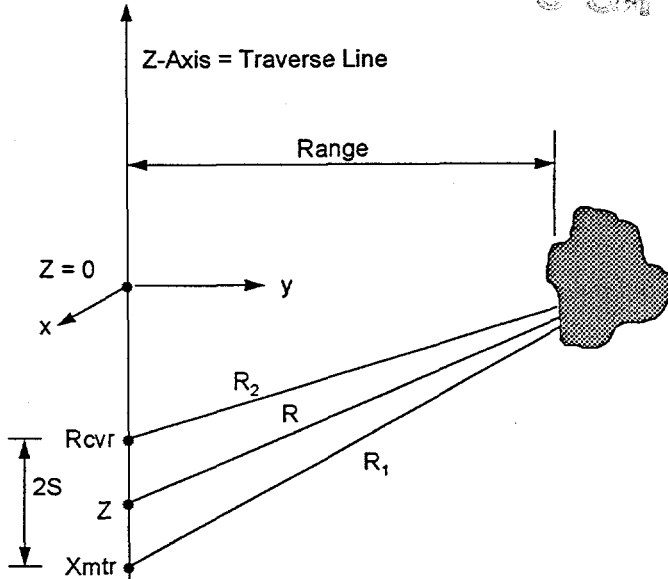


Figure 1. Traverse Geometry

The form of the trace generated with the traverse is obtained by equating (1) and (3), and using (2) to get

$$\frac{t_i^2}{t_o^2} - \frac{z_i^2}{\rho^2} = 1, \quad (4)$$

which is the standard form for an hyperbola centered at  $(z_i, t_i) = (0,0)$ .

From Fig. 1 it is simple to write the expression for the round-trip path length  $R_{n,i}$  in terms of  $R_i$ , namely

$$R_{n,i} = R_i \left\{ \sqrt{1 + \frac{\eta^2 + 2\eta\Gamma_i}{1 + \Gamma_i^2}} + \sqrt{1 + \frac{\eta^2 - 2\eta\Gamma_i}{1 + \Gamma_i^2}} \right\}, \quad (5)$$

<sup>o</sup> This work was supported by the United States Department of Energy under Contract DE-AC04-94AL85000.

#### **DISCLAIMER**

**Portions of this document may be illegible  
in electronic image products. Images are  
produced from the best available original  
document.**

## **DISCLAIMER**

This report was prepared as an account of work sponsored by an agency of the United States Government. Neither the United States Government nor any agency thereof, nor any of their employees, makes any warranty, express or implied, or assumes any legal liability or responsibility for the accuracy, completeness, or usefulness of any information, apparatus, product, or process disclosed, or represents that its use would not infringe privately owned rights. Reference herein to any specific commercial product, process, or service by trade name, trademark, manufacturer, or otherwise does not necessarily constitute or imply its endorsement, recommendation, or favoring by the United States Government or any agency thereof. The views and opinions of authors expressed herein do not necessarily state or reflect those of the United States Government or any agency thereof.

where  $\eta = s/\rho$  is the normalized separation distance, and  $\Gamma_i = |z_i|/\rho$  is the normalized traverse distance. We see from Fig. 2 that the error in using  $2R_i$  for the round-trip path length is greatest when  $z_i = 0$ , and that the separation distance should be made as small as possible.

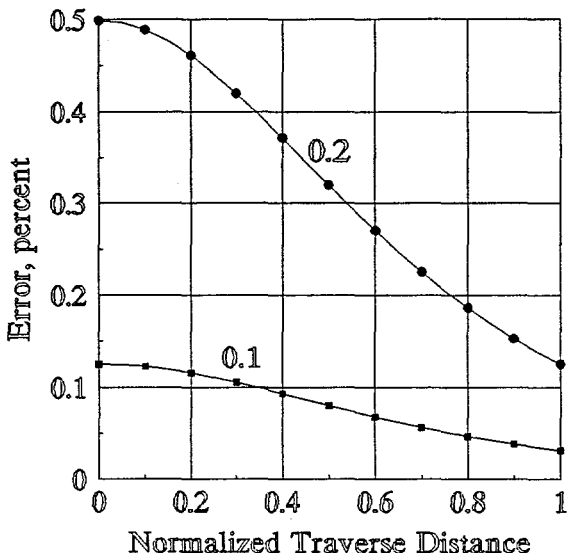


Figure 2. Midpoint error for  $\eta = 0.1, 0.2$

#### ALGORITHM DEVELOPMENT

The key idea in the algorithm consists in minimizing the difference between the propagation form for range, (1), and the Pythagorean form, (3), which is called the *difference function*:

$$DF = \left| \sqrt{z_i^2 + (v_j t_o / 2)^2} - v_j t_i / 2 \right|, \quad (6)$$

where the  $v_j$  are trial values of velocity,  $j = 1, 2 \dots j_{\max}$ .

The difference function is zero when  $t_i = t_o$ . I assume that, when the mean difference function is minimized over the set of trial velocities  $\{v_j\}$ , the velocity at the minimum will provide the range which is most consistent with the data.

The difference function may be set to zero and solved directly for as many trial velocities as there are data points. Often, the velocities thus found imply combinations of relative dielectric constant,  $RDC$ , and conductivity which are very different from any reasonable estimates of what the

electrical soil parameters could be. These so-called direct solution velocities are not used in the algorithm.

#### Constraints

The range-to-target algorithm is a numerical solution process and must be constrained to avoid instability, unwarranted precision, and results that are physically impossible. Because the difference method may require a large amount of computation and is subject to round-off errors, the  $(t_i, z_i)$ -data are read-in as double-precision numbers, and the computations are performed in double precision.

*Stability:* One problem arises from the limited precision of the time measurement itself. The several values of  $t_i$  in the vicinity of the apex of the hyperbola often have the same value, and the question arises as to which of these  $t_i$ -values should be designated as  $t_o$ . If the number of such values is odd, the middle value is chosen as  $t_o$ ; if the number is even, the mean value of the two  $t_i$  in the center is inserted as  $t_o$  together with a corresponding  $z_o$ . The  $z_i$  are subsequently recalculated so that only  $z_o = 0$ , and all other  $t_i$  equal to  $t_o$  are excluded from use in (6). This also increases the minimum values of the  $\Gamma_i$  and reduces the midpoint approximation error as shown in Fig. 2.

*Precision:* The uncertainty associated with each  $(z_i, t_i)$ -pair, namely  $\Delta z$  and  $\Delta t$ , can be used to estimate the relative error in the difference function, and to control the number of significant figures or *NSF* retained in the subtraction. The error in the trial velocities, which are computed values, is neglected.

The NSF to retain in the difference function is given by the characteristic of the common logarithm of the reciprocal of the relative error. If the NSF is one or more, only one or more significant figures are retained in the difference function; if the NSF is less than one, the difference function is not accumulated into the mean value. Consequently, it may turn out that the process of minimization may fail for lack of adequate precision.

*Velocity interval:* The difference function requires the use of trial velocities, and I assume that it is usually possible to make an estimate of the lower and upper limits of each of the electrical parameters. These are used to compute lower and upper bounds of the wavelength which, in turn, are used to provide bounds for the trial velocities. Alternatively, of course, the search could be conducted directly in terms of wavelength rather than velocity.

## EXAMPLES

Several examples are given below which demonstrate the usefulness of the algorithm in several different combinations of soils and targets. The first three examples use simulated data based on the return from a sphere [1], and the remaining six examples use field data taken by others on commercial equipment. The velocity search increment was 0.1% of the velocity interval in each example.

*Air Example:* The target is a 1m OD conductive sphere centered 50m from the traverse line. The transmitter and receiver are separated by 0.5m. The target RDC is also that of air, but the conductivity is 10mS/m. At a frequency of 100MHz the minimum round-trip time to the target surface is 330.2ns. The traverse extends  $\pm 0.85$ m in 0.1m intervals and provides extreme times of 330.3ns. Using just the extreme time on each side, 3 points in all, the estimated range is 49.49m which is very close to the minimum range-to-target distance of 49.5m.

*An Air Cavity in Granite:* The Boulder Creek granite formation near Raymond, Colorado has been extensively measured *in situ* at frequencies up to 25MHz [2]. At 12.5MHz the RDC is 7.8 and the conductivity is 1.8 mS/m which provide a wavelength of 8.47m and a velocity of 0.106 m/ns. A 1.6m-OD spherical cavity is centered 33m away. The transmitter & receiver are separated by 0.5m, and the traverse increment is 0.1m. Using data points between  $\pm 3.25$ m provides a range of 32.3m which is close to the minimum distance of 32.2m.

*A Saline Cavity in Granite:* This is the same as the previous example except that the target is changed to a 0.5m OD saline sphere centered at 9.64m. The target RDC is 81 and the conductivity is 180mS/m. Using data points between  $\pm 4.5$ m provides a range of 9.36m which is 3cm short of the minimum distance of 9.39m.

*Pipes and Barrels in Sand:* The January 1994 issue of *The EKKO Update*, a newsletter published by Sensors & Software, Inc., illustrated the responses from pipes and barrels buried at the GPR Antenna Range located at the University of Waterloo, Kitchener, Ontario. Fig. 3 shows the wiggle traces corresponding to five targets. All targets were buried at a depth of 1.30m in a uniform sand overlying a water table which began at a depth of 4m. The trace for the vertical barrel, the 4th target, is rather flat on top and does not extend as far along the traverse as the other traces because there is very little return from the vertical sides. A spurious response is also present at about 12m along the traverse. The trace for the horizontal barrel shows a minimum round-trip time which is about 1ns greater than

that of the other targets which suggests that the barrel is at a slightly greater depth. Sensors & Software, Inc. has kindly supplied the data which was acquired at 450MHz. The antenna separation of 0.25m made  $\eta \approx 0.1$  so that the midpoint approximation error of Fig. 2 is very small. The results of using the algorithm, with media search limits of  $5 \leq \text{RDC} \leq 10$ , and  $0.1\text{ms/m} \leq \text{Conductivity} \leq 1\text{mS/m}$ , are shown below.

Target Description	Depth, meters	Velocity, m/ns
0.5m steel cylinder	1.29	0.134
0.16m OD plastic pipe	1.25	0.130
0.16m OD steel pipe	1.28	0.133
Vertical barrel, 180L	1.31	0.134
Horizontal barrel, 180L	1.33	0.128

The differences between the computed and implanted depths are less than 4% for the first four targets. The horizontal barrel is about 3cm deeper than intended.

*Rebar Mesh in Concrete Slab on Grade:* In the January 1995 issue of *The EKKO Update*, Sensors & Software described the measurements shown in Fig. 4, and graciously provided a copy of the actual data obtained at 1200MHz. The antennas were separated by 7.5cm which was one-half the mesh spacing and one-half of the nominal slab thickness. The return at 1.2m along the traverse was investigated with media search limits of  $5 \leq \text{RDC} \leq 15$ , and  $0.01\text{ms/m} \leq \text{Conductivity} \leq 10\text{mS/m}$ . Times were only known to 2 significant figures, and the algorithm provided a depth of 11cm. This is consistent with both the traverse data and migrated image of Fig. 4 when using the algorithm velocity of 0.082m/ns and a minimum time of 2.7ns. The slab has not yet been bored to determine the actual depth of the mesh.

## CONCLUSIONS

The results given here are encouraging because of the variety of media parameters, frequency, and hyperbolic quality, but further testing is desirable. The algorithm appears to be ready for stand-alone use, or for integration into software associated with existing GPRs. It is worth noting that the algorithm is also applicable to seismic surveys with constant-offset gather.

## REFERENCES

- [1] H. W. March, "The field of a magnetic dipole in the presence of a conducting sphere," *Geophysics*, vol. 18, #3, pp. 671-684, July 1953.
- [2] R. N. Grubb, P. L. Orswell, and J. H. Taylor, "Borehole measurements of conductivity and dielectric constant in the 300 kHz to 25 MHz frequency range," *Radio Science*, vol. 11, #4, pp275-283, April 1976.

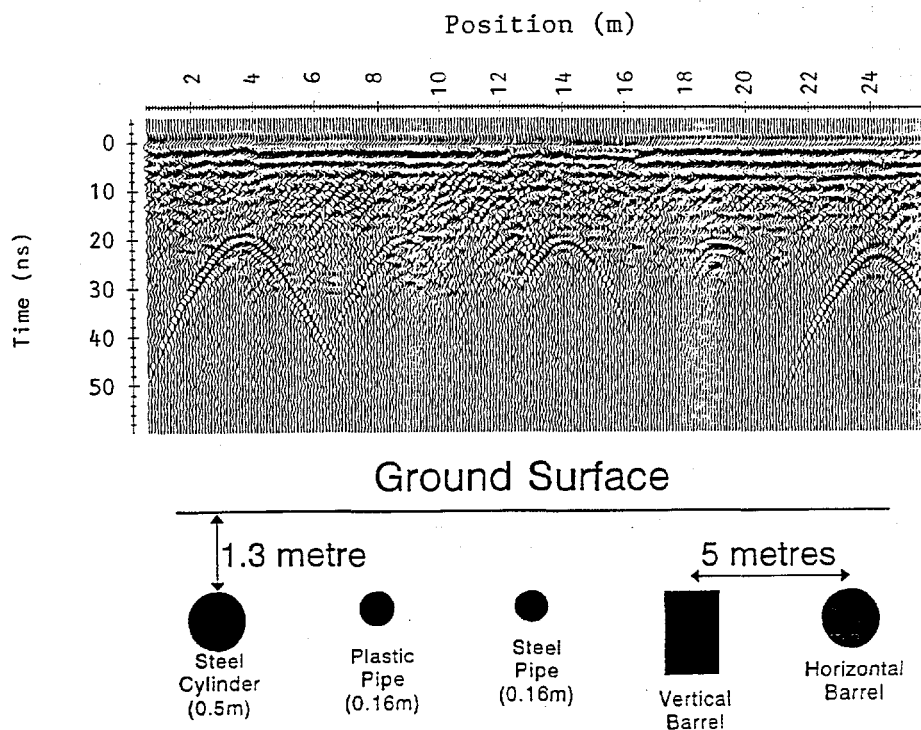


Figure 3. GPR returns at 450MHz at University of Waterloo GPR antenna test site

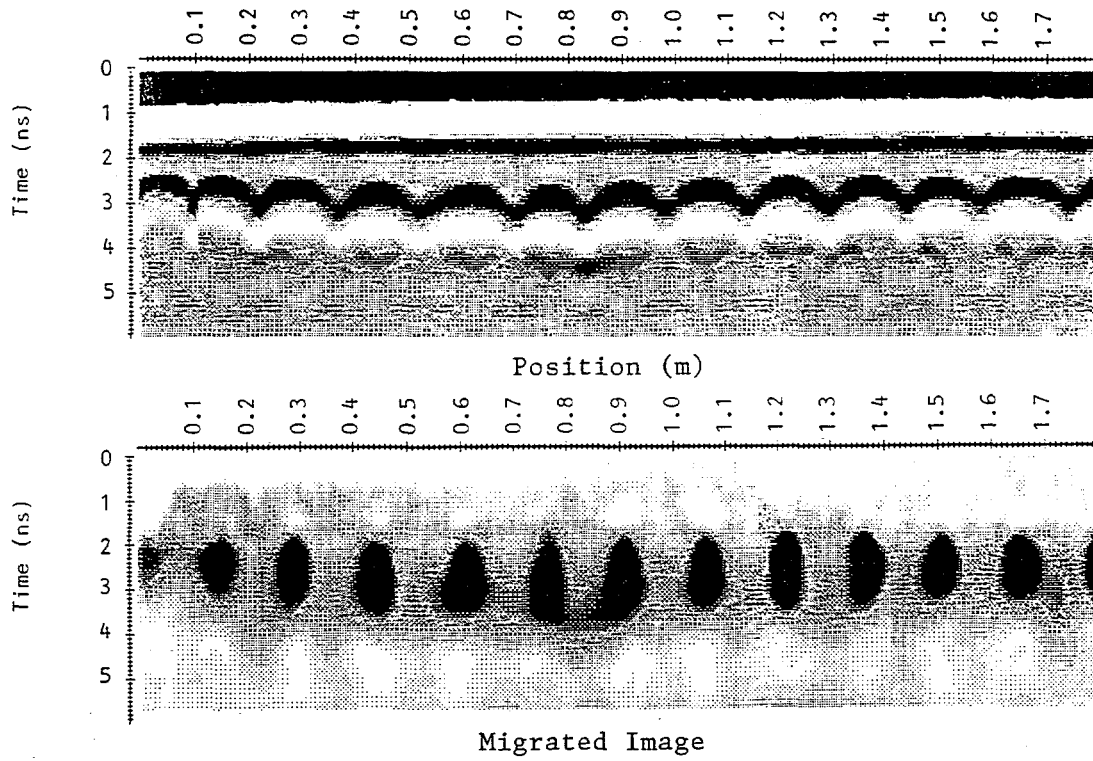


Figure 4. GPR returns at 1200MHz from rebar mesh in a concrete slab  
15mm x 15mm square mesh of 3mm wire in ~ 15cm thick slab